Methods of Constructing a Blended Performance Function Suitable for Formation Flight

John J. Ryan
*NASA Armstrong Flight Research Center, Edwards, California, 93523

This paper presents two methods for constructing an approximate performance function of a desired parameter using correlated parameters. The methods are useful when real-time measurements of a desired performance function are not available to applications such as extremum-seeking control systems. The first method approximates an a priori measured or estimated desired performance function by combining real-time measurements of readily available correlated parameters. The parameters are combined using a weighting vector determined from a minimum-squares optimization to form a blended performance function. The blended performance function better matches the desired performance function minimum than single-measurement performance functions. The second method expands upon the first by replacing the a priori data with near-real-time measurements of the desired performance function. The resulting blended performance function weighting vector is updated when measurements of the desired performance function are available. Both methods are applied to data collected during formation-flight-for-drag-reduction flight experiments.

Nomenclature

$\mathbf{A}_{(\cdot)}$	quadratic coefficient of an elliptic paraboloid
$\mathbf{B}$	blended performance function
$\mathbf{b}_{(\cdot)}$	linear coefficient of an elliptic paraboloid
$\mathbf{D}$	desired performance function parameter
$\mathcal{D}$	mapping of independent variable to desired performance function
i	index of parameter maps $\mathcal{P}$
l	size of independent variable vector index $\mathbf{x}$
m	range of index i
n	number of instances of $\mathbf{x}$ in $\mathbf{X}$
$\mathbf{P}$	dependent parameters
$\mathcal{P}_i$	mapping of independent parameter to dependent parameters
V	weighting factor
$\mathbf{X}^*_{(\cdot)}$	extremal coordinates
$\mathbf{X}$	discrete set of independent variable vectors
$\mathbf{x}$	independent variable vector

I. Introduction

This paper proposes two methods of approximating a performance function of a desired parameter using correlated parameters. The methods are useful when real-time measurements of a desired performance function are not available in real time for applications such as extremum-seeking control. Instead, values of available correlated parameters are measured and linearly combined through a weighted least-squares method to approximate the desired performance function. The extremum of the blended performance function approximates the coordinates of the extremum of the desired performance function more closely than performance functions formed from individual correlated parameters. Both methods are illustrated with an

*Aerospace Engineer, Controls and Dynamics Branch, P.O. Box 273/Mailstop 4840D, AIAA Member.

example. This work is motivated by the lack of readily available fuel-flow measurements in the formation-flight-for-drag-reduction problem.

The main contribution of this paper is the introduction of two methods to construct blended performance functions which approximate desired performance functions when they are not available for use. This paper begins by introducing the two methods. Section 2 develops an a priori weighting method. Section 3 develops a second method in which the weighting vector is updated over time. Section 4 provides an overview of formation flight for drag reduction. Section 5 applies the two methods to the formation-flight-for-drag-reduction problem. Section 6 concludes the paper.

II. A Priori Weighting

The first method of constructing blended performance functions linearly combines readily available measurements with an a priori calculated optimal weighting vector. Define mappings of independent variable vector $\mathbf{x} \in \mathbb{R}^l$ to the desired performance function $\mathcal{D} : \mathbf{x} \to D \in \mathbb{R}$. It is assumed that while measurements of D are not available in real time, a priori values of D are available. Also define a discrete set, $\mathbf{X} \subset \mathbb{R}^{l \times n}$ of n instances of $\mathbf{x}$. Further define mappings of $\mathbf{x}$ to parameters P_i, $\mathcal{P}_i : \mathbf{x} \to P_i \in \mathbb{R}$. It is assumed that each $\mathcal{P}_i$ is correlated to $\mathcal{D}$. Here i is an index ranging from 1 to m where m is the total number of parameters. Define the discrete set $\mathbf{P} = \left[\mathcal{P}_1(\mathbf{X})^T, \mathcal{P}_2(\mathbf{X})^T, \ldots, \mathcal{P}_m(\mathbf{X})^T\right]^T$. A blended performance function is defined as

$$\mathbf{B} = \mathbf{wP} \tag{1}$$

where $\mathbf{w} \in \mathbb{R}^m$ is a weighting vector. It is assumed that $\mathbf{P}$ has full column rank. It is further assumed that $\mathbf{X}$ is chosen such that each mapping is convex. This assumption ensures the blended performance function is convex as shown by Boyd.[1]

A generalized least-squares problem is solved to determine the optimal weighting $\hat{\mathbf{w}}$, which minimizes the error between the sets $\mathcal{D}(\mathbf{X})$ and $\mathbf{B}$

$$\hat{\mathbf{w}} = \arg_{\mathbf{w}} \min \Big(\mathcal{D}(\mathbf{X}) - \mathbf{wP}\Big)^T V^{-1} \Big(\mathcal{D}((\mathbf{X}) - \mathbf{wP}\Big). \tag{2}$$

The restrictions on $\mathbf{X}$ ensure a solution to the least-squares problem exists. With the assumption that the extremum of $\mathcal{P}_i$ surround that of $\mathcal{D}(\mathbf{X})$, the nonsingular weighting factor V is chosen to ensure the extremum coordinates of $\mathbf{B}$ closely match the extremum coordinates of $\mathcal{D}(\mathbf{X})$.

III. Weight Updating

The second method of constructing a performance function is an augmentation of the first. It also linearly combines measurements in order to form a blended performance function but updates the weighting vector $\hat{\mathbf{w}}$ as the system evolves in time. This requires estimates of the shape of the desired performance function. The estimates are assumed to be much to be much slower than the measurements of $\mathbf{P}_i$.

The method assumes that the mappings $\mathcal{D}$ and $\mathcal{P}_i$ can be approximated as elliptic paraboloids:

$$\mathcal{D} = \frac{1}{2} X^T \mathbf{A_D} X + X^T \mathbf{b_D}$$
$$\mathcal{P}_i = \frac{1}{2} X^T \mathbf{A}_i X + X^T \mathbf{b}_i$$

Any other unimodal functional may be equivalent used. The values of $\mathbf{A}_{(\cdot)}$, $\mathbf{b}_{(\cdot)}$ are found with a time-varying Kalman filter as presented in Ryan.[2] The subscripts of $\mathbf{A}$ and $\mathbf{b}$ indicate the parameter to which each is associated.

As the system evolves in time, periodic measurements of the desired performance function $\mathbf{D}$ are made. In practice, these non-real-time measurements may require a dwell-time or averaging in order to obtain steady-state measurements. The values of $\mathbf{A_D}$, and $\mathbf{b_D}$ are then updated and $\hat{\mathbf{w}}$ is calculated with Eq. 2.

In between measurements of the desired performance function, $\mathcal{P}_i$ measurements continue to be made and $\mathbf{A}_{(\cdot)}$ and $\mathbf{b}_{(\cdot)}$ are updated as described by Ryan.[2] The blended performance function $\mathbf{B}$ is updated according to Eq. 1.

The extremum coordinates of $\mathcal{P}_i$ must surrounded that of $\mathcal{D}$ to ensure the method is feasible. With the elliptic paraboloid implementation, the blended function of Eq. 1 is written as:

$$\mathbf{B} = \sum_{i=1}^{m} \mathbf{w}_i \left(\frac{1}{2} X^T \mathbf{A}_i X + X^T \mathbf{b}_i \right).$$

The extremum coordinate of $\mathbf{B}$ is easily determined to be

$$X^*_{\mathbf{B}} = \left[\sum_{i=1}^{m} \mathbf{w}_i \mathbf{A}_i \right]^{-1} \sum_{i=1}^{m} \mathbf{w}_i \mathbf{b}_i. \tag{3}$$

Using the fact that the extremum coordinate for each contributing elliptical paraboloid is given by

$$X^*_{(\cdot)} = -A_i^{-1} b_i$$

Eq. 3 is written as:

$$X^*_{\mathbf{B}} = \left[\sum_{i=1}^{m} w_i A_i \right]^{-1} \sum_{i=1}^{m} w_i A_i X^*_i.$$

Hence $X^*_{\mathbf{B}}$ is the weighted mean of the set of X^*_i with the weights determined by $\mathbf{w}_i \mathbf{A}_i$. The elemental functions must therefore be chosen such that the properties of a weighted mean are satisfied such as boundedness:

$$\min X^*_i < X^* < \max X^*_i$$

which indicates the extremum coordinates of $\mathcal{P}_i$ must surround that of $\mathcal{D}$.

When the blended performance functions are to be used in extremum-seeking control, it must also be assured that $\mathbf{B}$ remains convex during updates. If $\mathbf{B}$ does not remain convex, the extremum-seeking control may drive the system away from the optimal location. Boyd[1] (page 79) shows that a nonnegative weighted sum of convex functions is also convex. The assumption of a elliptic paraboloid form therefore ensures $\mathbf{B}$ will remain convex as long as each $\mathcal{P}_i$ is convex. This assumption is easily enforced in practice by checking the Hessian of $A_{(\cdot)}$.

IV. Formation Flight for Drag Reduction

The methods of approximating a performance function discussed in sections II and III were developed to address the lack of available measurements of fuel savings in the formation-flight-for-drag-reduction problem. Formation flight for drag reduction provides significant fuel savings for a formation of aircraft; it is an active area of research examined from various perspectives in works by Okolo,[3] Kniffen,[4] Beukenberg,[5] Ning,[6] Bower,[7] and others.

In a formation of two aircraft, the trailing aircraft is positioned such that one wing resides in the upwash created by the wingtip wake vortices of the leading aircraft. This position is typically realized with the wingtip of the trailing aircraft residing near the core of the wingtip wake vortex of the leading aircraft, as seen in Fig. 1.

Additional effects, such as induced rolling moment, pitching moment, and yawing moment, are introduced on the trailing aircraft due to interaction with the vortex. The strength of these effects depends upon the relative positions of the aircraft in the formation. Effects on the leading aircraft are typically negligible at relative positions with nose-to-tail separation.

Conceptual designs of an automatic control system intended to realize formation flight for drag reduction may employ an extremum-seeking control system to optimize the fuel-savings benefits. Examples of such systems are found in work by Ryan,[2] Chichka,[8] and Binetti.[9] Each of these systems estimates the local gradient of a performance function and commands the trailing aircraft of the formation to a relative position which minimizes the gradient of the performance function.

Ideally, such a formation flight control system would employ a performance function formed from measurements of fuel flow, thereby directly minimizing the fuel used during flight. Unfortunately, fuel-flow measurements possess undesirable characteristics which limit their usefulness, partially because of the response time of engine response to throttle commands. The Code of Federal Regulations, Part 33, Section

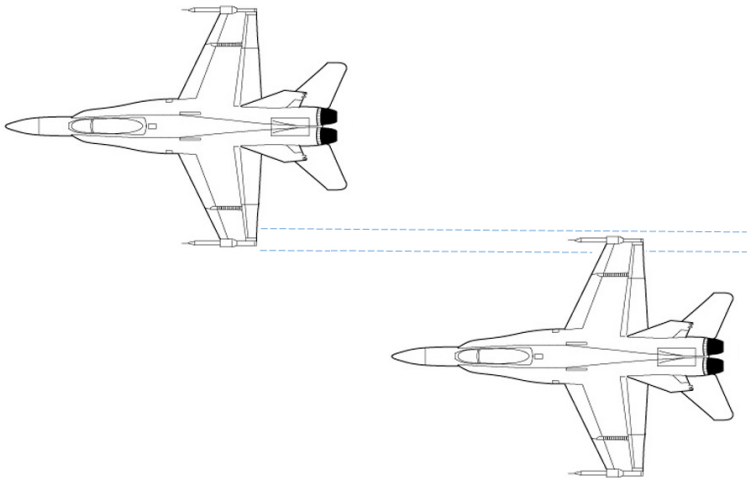

Figure 1. Two aircraft in formation flight with the trailing aircraft's wingtip in the wingtip vortex of the leading aircraft.

33.73 requires an engine to enable an increase from not more than 15% thrust available to 95% thrust in not over five seconds. It is reasonable to expect the engine response, and therefore fuel-flow response, to be no faster than this.

Many approaches sidestep this issue by extremizing performance functions formed from measurements analogous to fuel flow. For example, Lavretsky[10] minimizes throttle activity, Chichka[8] maximizes the induced rolling moment, and Binetti[9] maximizes the induced pitch angle. With each of these approaches, the extremum-seeking control system improves the fuel savings achieved; however, each approach has limitations. The true fuel-flow extremum coordinates do not necessarily coincide with that of the analogous measurement, and the measurement may possess undesirable characteristics such as significant lag.

V. Application to Formation Flight for Drag Reduction

The methods discussed in sections II and III are applied to data derived from flight experiments of two F/A-18 aircraft (McDonnell-Douglas, now The Boeing Company, Chicago, Illinois) in formation reported by Vachon,[11] and Hansen.[12] The data consist of changes in fuel flow, drag, rolling moment, yawing moment, pitching moment, and side force as a function of changes in relative vertical, lateral, and longitudinal positioning. In this work, only the changes in relative vertical and lateral positioning are considered.

Assign the relative position between aircraft as the independent variable $\mathbf{x}$. Assign rolling moment, pitching moment, and yawing moment to the parameters $\mathbf{P}_i$. Further assign fuel flow as the desired performance function $\mathcal{D}$. For purposes of this example, and because the data were available, it is assumed that rolling moment, pitching moment, and yawing moment are readily measurable. In application, other correlated parameters may be more appropriate. Figure 2 depicts normalized fuel flow, rolling moment, pitching moment, and yawing moment as functions of relative position between aircraft. Rolling moment, pitching moment, and yawing moment as depicted in Figs. 2(b), 2(c), and 2(d) resemble fuel flow as depicted in Fig. 2(a). Each is unimodal with different extremum coordinates. The relative position set $\mathbf{X}$ was selected to ensure the sets $\mathbf{P}_i$ are convex. A blended performance function was formed by linearly combining the rolling-moment, pitching-moment, and yawing-moment performance functions with weights calculated from Eq. 2 and choosing $V = I$ results in the weighting vector

$$\hat{w} = \begin{bmatrix} 1.3 & 1.1 & -1.2 \end{bmatrix}. \tag{4}$$

Figure 3(a) depicts the blended surface. Figure 3(b) depicts the extrema locations of the drag-reduction, rolling-moment, pitching-moment, yawing-moment, and blended performance functions. It is clear that the blended performance function extremum is nearer that of drag reduction than the other performance functions.

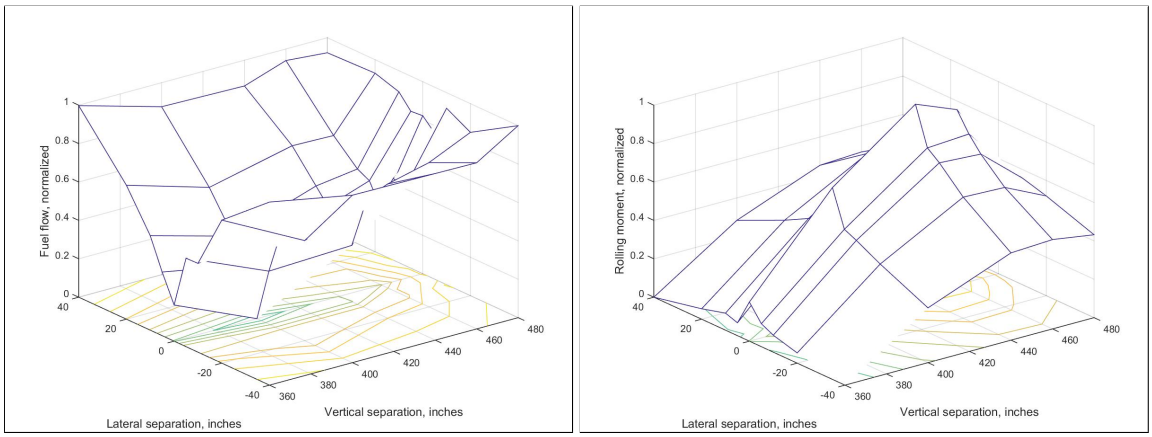

(a) Normalized fuel flow

(b) Normalized rolling moment

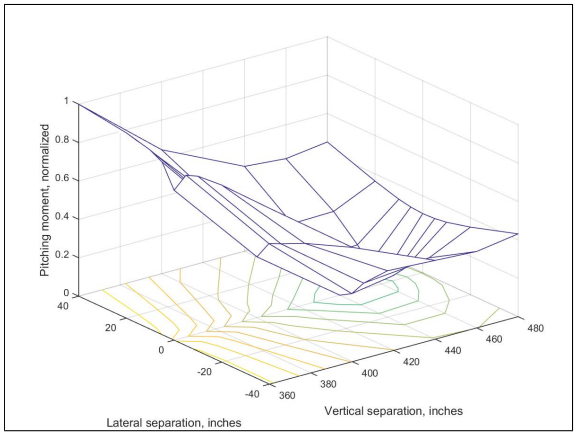

(c) Normalized pitching moment

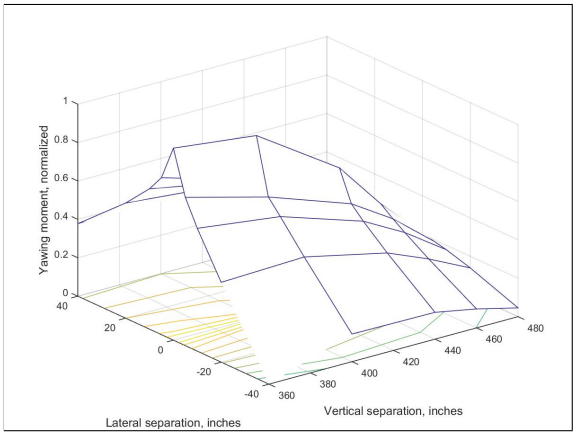

(d) Normalized yawing moment

Figure 2. Normalized fuel flow, rolling moment, pitching moment, and yawing moment data used to construct a blended performance function.

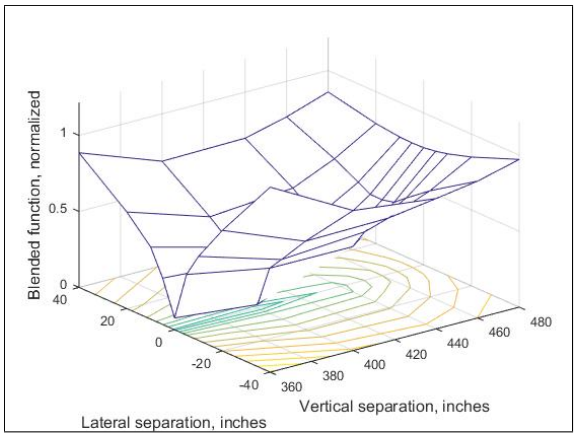

(a) Blended performance function surface

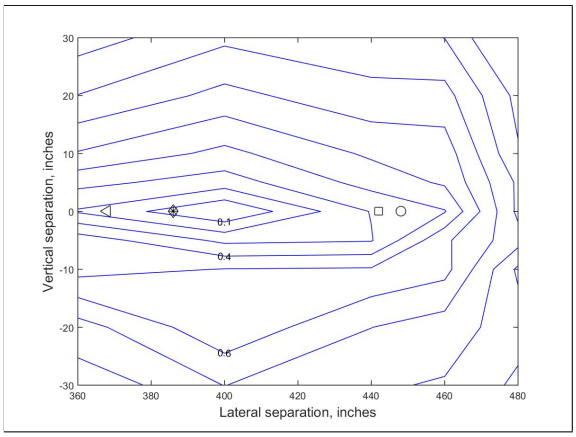

(b) Blended performance function contour

Figure 3. Blended performance function and extremum locations of fuel flow (∗), rolling moment (□), pitching moment (○), yawing moment (◁), and blended function (◇).

The main limitation of this method is the restriction to an a priori calculation of $\hat{w}$. If $\mathcal{D}$ is not an accurate representation of the actual performance function, then $\mathcal{B}$ will not provide a good indication of the extremum coordinates. Similarly, if the relationships between $\mathcal{P}_i$, and D are not accurate or are not constant over time, then the extremum coordinates will not be found.

The second method was applied to the flight experiment data described above. Figure 4 displays contours of the performance functions and the parabolic functions to which they were fit. Figure 4(a) shows the fuel flow contour; 4(b) the rolling moment contour; 4(c) the pitching moment contour; and 4(d) the yawing moment contour.

Figure 5 displays the fuel-flow performance function, the blended performance function, and the extremal locations of fuel flow, rolling moment, pitching moment, yawing moment, and the blended performance function. Figure 5(a) indicates the blended performance function matches the shape of the fuel flow performance function in the area around the extremum. Figure 5(b) indicates that the extremum of the blended performance function more closely matches that of fuel flow than the other individual parameters.

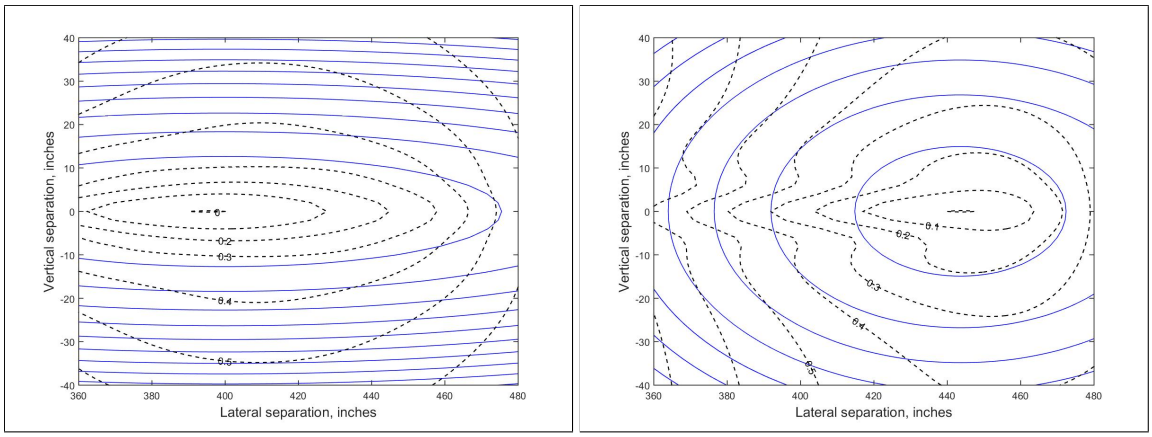

(a) Fuel flow performance function

(b) Rolling moment performance function

(c) Pitching moment performance function

(d) Yawing moment performance function

Figure 4. Contour plots of performance functions (dashed lines) and their parabolic fitted performance functions (solid lines).

The main limitation of this method is the requirement of a dwell-time for fuel flow measurements, which slows the convergence of the extremum-seeking control system. A second limitation is the increased computational burden over the first method. Kalman filters are required to estimate the shape of each component function $\mathcal{P}_i$ at each time step and the fuel flow function after each fuel flow measurement.

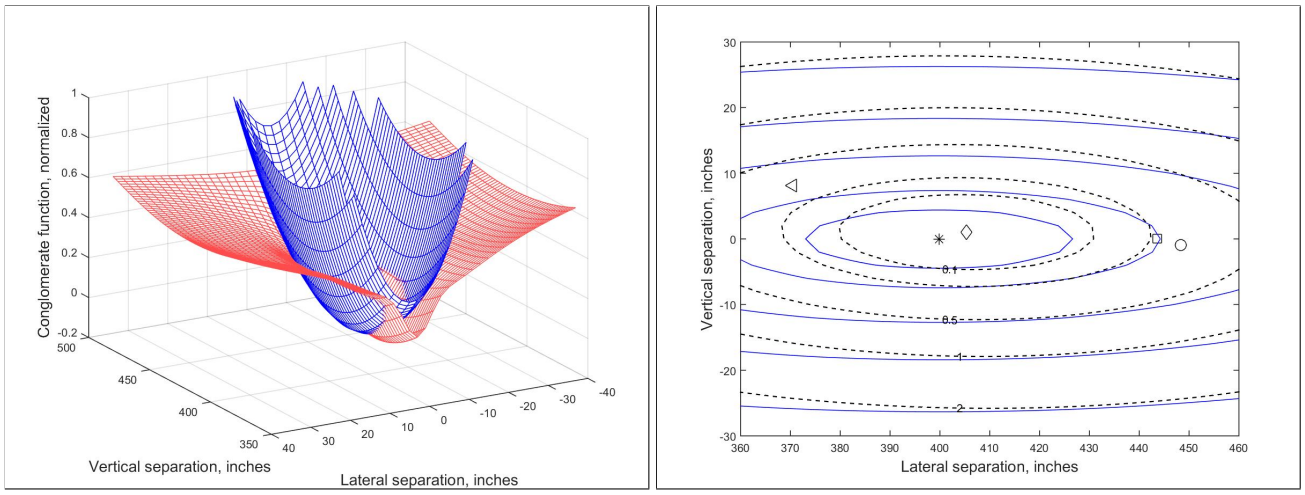

(a) Fuel flow optimization

(b) Fuel flow performance function

Figure 5. Minimum locations of the individual functions and of the blended performance function along with contour plots of the fuel-flow performance function(solid lines) and the blended performance function (dashed lines); fuel flow($\ast$), rolling moment ($\square$), pitching moment ($\circ$), yawing moment ($\triangleleft$), and blended function ($\diamond$).

VI. Conclusion

Two methods of approximating a performance function using correlated parameters are shown and applied to the problem of formation flight for drag reduction. Both methods utilize readily available measurements to form a blended performance function which approximates that of the desired performance function. The first method uses a priori measurements to determine a weighting vector which is applied to real-time measurements in forming the performance function. The second method periodically updates the weighting vector by fitting elemental functions to measurements of fuel flow. Future work will examine these methods in a time-based formation-flight simulation to confirm effectiveness of the methods.

References

[1]Boyd, S. and Vandenberghe, L., *Convex Optimization*, Cambridge University Press, 2004.

[2]Ryan, J. J. and Speyer, J. L., "Peak-Seeking Control Using Gradient and Hessian Estimates," *American Control Conference (ACC)*, 2010, pp. 611–616.

[3]Okolo, W., Dogan, A., and Blake, W., "Effect of Trail Aircraft Trim on Optimum Location in Formation Flight," *Journal of Aircraft*, Vol. 52, No. 4, 2014, pp. 1201–1213.

[4]Kniffin, C., Dogan, A., and Blake, W. B., "Formation Flight for Fuel Saving in Coronet Mission - Part A: Sweet Spot Determination," AIAA-2016-3393, 2016.

[5]Beukenberg, M. and Hummel, D., "Aerodynamics, Performance and Control of Airplanes in Formation Flight," ICAS-90-5.9.3, 1990.

[6]Ning, A., Flanzer, T. C., and Kroo, I. M., "Aerodynamic Performance of Extended Formation Flight," AIAA-2010-1240, 2011.

[7]Bower, G. C., Flanzer, T. C., and Kroo, I. M., "Formation Geometries and Route Optimization for Commercial Formation Flight," AIAA-2009-3615, 2009.

[8]Chichka, D. F., Speyer, J. L., Fanti, C., and Park, C. G., "Peak-Seeking Control for Drag Reduction in Formation Flight," Vol. 29, 2006, pp. 1221–1230.

[9]Binetti, P., Ariyur, K. B., Krstic, M., and Bernelli, F., "Formation Flight Optimization Using Extremum Seeking Feedback," *Journal of Guidance, Control, and Dynamics*, Vol. 26, No. 1, 2003, pp. 132–142.

[10]Lavretsky, E., Hovakimyan, N., Calise, A., and Stepanyan, V., "Adaptive Vortex Seeking Formation Flight Neurocontrol," AIAA-2003-5726, 2003.

[11]Vachon, M. J., Ray, R. J., Walsh, K. R., and Ennix, K., "F/A-18 Aircraft Performance Benefits Measured During the Autonomous Formation Flight Project," AIAA-2003-4491, 2002.

[12]Hansen, J. L. and Cobleigh, B. R., "Induced Moment Effects of Formation Flight Using Two F/A-18 Aircraft," AIAA-2002-4489, 2002.